NASA TM- 84525

NASA-TM-84525 19820025861

NASA Technical Memorandum 84525

IMPROVED DAMAGE TOLERANCE OF TITANIUM BY ADHESIVE LAMINATION

W. S. Johnson

July 1982

NASA
National Aeronautics and
Space Administration

Langley Research Center
Hampton, Virginia 23665

IMPROVED DAMAGE TOLERANCE OF TITANIUM BY ADHESIVE LAMINATION

W. S. Johnson
Research Engineer
NASA Langley Research Center
Hampton, Virginia 23665

ABSTRACT

Basic damage tolerance properties of Ti-6Al-4V titanium plate can be improved by laminating thin sheets of titanium with adhesives. Compact tension and center-cracked tension specimens made from thick plate, thin sheet, and laminated plate (six plies of thin sheet) were tested. The fracture toughness of the laminated plate was 39 percent higher than the monolithic plate. The laminated plate's through-the-thickness crack growth rate was about 20 percent less than that of the monolithic plate. The damage tolerance life of the surface-cracked laminate was 6 to over 15 times the life of a monolithic specimen. A simple method of predicting crack growth in a crack ply of a laminate is presented.

INTRODUCTION

Titanium is a desirable material for aerospace applications primarily because of its high strength-to-weight ratio and high temperature stability. However, as shown by Elber and Davidson [1], titanium's usefulness is limited by the small size of tolerable initial flaws and the rapidity by which they grow. The purpose of this paper is to show how Ti-6Al-4V titanium's toughness can be increased, the crack growth rate decreased, and the overall damage tolerance significantly improved by adhesive lamination.

Previous research [2-6] has demonstrated that adhesively bonding thin sheets of aluminum together improved the toughness and damage tolerance. The higher toughness is attributed to the individual thin plies failing in plane stress, instead of plane strain as a monolith of the same plate thickness would [2]. The improved damage tolerance is attributed to two mechanisms: (1) the crack in a single ply, when restrained by uncracked plies, has a longer crack life than the same crack in a monolith [4], and (2) the crack in one ply cannot easily grow past the adhesive into the adjacent uncracked ply [4,6]. The latter situation makes for a "fail-safe" structure.

Recent U.S. Air Force sponsored programs have shown the relative advantages in cost, weight, and damage tolerance of adhesively bonded joints and laminated aluminum wing skins over traditional methodology using mechanical fasteners [7,8]. The laminated aluminum design was even judged superior to some composite wing designs [7]. These U.S. Air Force sponsored programs were highly successful in demonstrating the advantages of adhesively bonded structures (including the PABST program [9]) and adhesively bonded laminated wing skins in particular; however, virtually no U.S. aircraft has yet incorporated these concepts. Meanwhile, Fokker-VFW B.V. of The Netherlands has been adhesively bonding primary structures for 30 years with great success [10,11]. They used laminated aluminum extensively, particularly for lower wing skins. They have achieved low fabrication costs, low structural weight, little material waste, and economical operation through the extensive use of adhesives, plus millions of hours of successful flight time.

This paper shows that titanium monolithic properties such as toughness, crack growth resistance, and damage tolerance are improved significantly by adhesively bonding thin plies of titanium together to form a laminate. This study will also serve to expand the present data base that consists primarily of bonded aluminums.

Thin sheet, monolithic plate, and adhesively bonded laminated plate of Ti-6Al-4V material were tested using compact, center-cracked tension, and surface-cracked tension specimens. The fracture toughness and crack growth properties are compared for the three titanium material systems (thin sheet, thick plate, and laminated plate). The damage tolerance, crack growth, and life were compared for monolithic and laminated plate specimens of the same approximate thickness. Analysis was used to interpret the toughness data and to predict crack growth in laminates.

LIST OF SYMBOLS

a	crack length in compact tension specimen; half crack length in center-cracked tension specimen
C	crack growth constant
f	boundary correction factor
$f(a/w)$	boundary correction factor for compact tension specimen
f_ℓ	stress-intensity correction factor for the adhesive lamination
K_c	critical stress-intensity factor, MPa$\sqrt{mm}$
m	crack growth constant
N	number of applied cycles
N_p	number of plies in a laminate
n	crack growth constant
P	load, kN
P_c	critical failing load, kN
P_{eff}	effective load in cracked ply of a laminate
R_b	ratio of induced tensile bending stress in the cracked ply to the average remote tensile stress
R_{eff}	effective stress ratio used in crack growth equation
S_{eff}	effective remote stress in a cracked ply of a laminate without bending
$(S_{tot})_{eff}$	effective remote stress in a cracked ply of a laminate including bending
t	thickness of ply
w	width of specimen
ΔK	stress-intensity factor range
ΔK_{TH}	threshold stress-intensity factor range

ΔK^{o}_{TH} threshold stress-intensity factor range at $R = 0$

ΔP applied load range

ΔS applied stress range

λ a/w

EXPERIMENTS

Three material systems are examined in this investigation: (1) thin (1.27 mm) sheet material like that used in the laminate, (2) thick (9.91 mm) monolithic plate material, and (3) thick (8.89 mm) laminated plate consisting of six plies of 1.27-mm-thick sheet. All material is Ti-6Al-4V beta annealed. The thin sheets and the thick monolithic plates were tested for hardness (Rockwell) at numerous locations to ensure that they were both annealed to similar conditions. Therefore, it is assumed that they are both the same material--only differing in thickness.

Six plies of the sheet material were adhesively bonded together with AF-147 to form a plate 460 mm square. The adhesive was cured at 450 K for one hour under 0.31 MPa pressure. The resulting laminate plate thickness was 8.89 mm. Each bond-line was approximately 0.25 mm thick.

Compact specimens of the dimensions shown in Fig. 1 were machined from the laminated plate, the monolithic plate, and the thin sheets. Center-cracked tension specimens, as shown in Fig. 2, were machined out of the thin sheet. Surface-cracked tension specimens of the same dimensions shown in Fig. 2 were machined from the thick monolithic and laminated plates. The initial surface flaw was semicircular and made by electronic discharge machining (EDM).

All crack growth rate and fatigue tests were conducted at a frequency of 10 cycles per second. Electrohydraulic testing machines were used. All machined or eloxed cracks were precracked under constant-amplitude loading before the actual crack growth tests were conducted. Crack length was measured optically or by electric foil resistance gages. Usually the number of cycles applied was recorded at every 0.64 mm increment of crack growth. A three-point incremental polynomial method was used to determine crack growth rate (da/dN) from the crack length against number of cycles data, as described in ASTM Standard E647 [12].

Specimen loads were calculated so that the load on a laminated specimen had the same ratio of load to weight as that used on a monolithic specimen. This was true for all load levels. The density of the adhesive plus scrim cloth was assumed to be one-third that of titanium. The thickness ratio of the laminate to the monolith is 1.11. For equal load-to-weight ratios, load in the laminate equals 0.81 times the load in the monolith.

ANALYSIS

This section describes the stress-intensity factor equations used for the compact tension (CT) and the center-cracked tension (CCT) specimens. A crack growth rate equation used to describe constant-amplitude results is also presented. Furthermore, a simple algorithm for predicting crack growth in a cracked outer ply of a laminate is discussed.

Stress-Intensity Factors

The equations for the stress-intensity factor range, ΔK, and critical stress-intensity, K_c, for a CT specimen [13] are

$$\Delta K = \left(\Delta P/tw^{1/2}\right)f(a/w) \tag{1a}$$

and

$$K_c = \left(P_c/tw^{1/2}\right)f(a/w) \tag{1b}$$

where

$$f(a/w) = \frac{(2 + \lambda)\left(0.886 + 4.64\lambda - 13.32\lambda^2 + 14.72\lambda^3 - 5.6\lambda^4\right)}{(1 - \lambda)^{3/2}}$$

and

$\lambda = a/w$

ΔP = applied load range

P_c = failure load

t = specimen thickness

a = crack length

w = specimen width

The equation for the stress-intensity factor range, ΔK, for a CCT specimen [14] is

$$\Delta K = S(\pi a \sec(\pi a/w))^{1/2} \tag{2}$$

where

S = applied stress range

a = half length of crack

Crack Growth Rate Equation

In order to predict the crack growth behavior of a cracked outer ply of a laminated specimen the crack growth behavior of the thin sheet must be known. The equation used to describe the crack growth rate (da/dN) for the thin sheet Ti-6Al-4V is

$$\frac{da}{dN} = \frac{C\left(\Delta K^2 - \Delta K_{TH}^2\right)^n}{\left(1 - R_{eff}\right)^m K_c - \Delta K} \tag{3}$$

where

$\Delta K_{TH} = \left(1 - R_{eff}\right) \Delta K_{TH}^o$

ΔK_{TH}^o = threshold stress-intensity factor at $R = 0$

$R_{eff} = R$ if $R \leq 0.5$

$R_{eff} = 0.5$ if $R > 0.5$

$m = 1$ if $R \geq 0$

$m = 2$ if $R < 0$

K_c = critical stress-intensity factor

$\left.\begin{array}{l} C = \\ n = \end{array}\right\}$ material dependent parameters

This equation has the basic form suggested by Forman [15]. Chu [16] suggested putting the ΔK_{TH} in the numerator. The equation is further modified to let ΔK_{TH} vary with R, and has the $(1 - R)$ term raised to the second power for negative R values [17]. The total ΔK range is used when $R < 0$ (not just the tensile stress portion). This equation has been used to model crack growth data for 10-nickel steel, 2219-T851, and 7075-T651 aluminum alloys very successfully at positive and negative stress ratios. The values C, n, ΔK^o_{TH}, and K_c are material dependent.

Laminate Crack Growth Algorithm

To predict how a crack in an outer ply grows, the stress in the cracked ply must be defined and the influence of the adhesive bond evaluated. Roderick [18] and Ratwani [19] have performed rigorous analyses using a continuum mechanics approach and a finite-element analysis, respectively, and a complete characterization of the adhesive debond behavior for the adhesively bonded laminates. In the present paper, the author has chosen to take a less rigorous, somewhat empirical, approach like that in Refs. 4 and 5. This approach is simple and handy for designers to evaluate a given material system. Bending is induced as the crack in an outer ply grows [4] because the laminate's cross section becomes unsymmetric. Equations for the stress in the cracked ply due to axial load and the induced bending moment have been determined for laminated aluminum and presented previously [4,5]. The equations are summarized below.

The effective axial load $\left(P_{eff}\right)$ in the cracked ply is

$$P_{eff} = \frac{\text{Net area of cracked ply}}{\text{Net area of cracked section}} \times P$$

therefore,

$$P_{eff} = \frac{w - 2a}{N_p w - 2a} \times P \tag{4}$$

where

P = applied load to specimen

N_p = number of plies

The effective remote stress $\left(S_{eff}\right)$ in the cracked ply due to axial load transfer is

$$S_{eff} = \frac{P_{eff}}{wt} \tag{5}$$

Equations (4) and (5) assume that uniform strain exists across the cracked section and that all plies have the same thickness and width.

The effective bending stress for the 6-ply laminate was extrapolated from 2-, 3-, and 4-ply data [4]. The ratio, R_b, of induced tensile bending stress in the cracked ply to the average remote tensile stress can be expressed as a function of crack length, 2a, to specimen width, w, for a given specimen geometry. The assumed equation for a 6-ply laminate is

$$\left.\begin{array}{ll} R_b = [2(a/w) - 0.3] \times 0.33 & 2a/w > 0.3 \\ R_b = 0 & 2a/w \leq 0.3 \end{array}\right\} \tag{6}$$

Thus, the total "effective" remote stress acting on the cracked ply in a finite-width specimen is

$$\left(S_{tot}\right)_{eff} = S_{eff}\left(1 + R_b\right) \tag{7}$$

The crack in an outer ply of the laminate was assumed to be a through-crack in a finite-width thin sheet with a remote stress of $\left(S_{tot}\right)_{eff}$. Therefore, the stress-intensity factor range for the crack became

$$\Delta K = \Delta\left(S_{tot}\right)_{eff}(\pi a \sec(\pi a/w))^{1/2} f_{\ell} \tag{8}$$

where f_{ℓ} is the correction factor for the adhesive lamination. This was substituted into equation (3) to predict the crack growth behavior for the crack in a single ply of a laminate subjected to constant-amplitude loadings.

RESULTS AND DISCUSSION

This section presents the experimental and, where applicable, the analytical results. It is divided into four parts: through-the-thickness crack growth, fracture toughness, thin sheet crack growth, and laminate damage tolerance.

Compact specimens were used to assess two areas of material behavior: (1) comparison of through-the-thickness crack growth rates under constant-amplitude loading for the thin sheet, thick monolith, and laminated plate, and (2) comparison of through-the-thickness fracture toughness for the three material systems.

The surface-cracked tension specimens were used to study crack growth in cracked plies bonded to uncracked plies and to study the total life of surface-cracked specimens. Crack growth and life for laminates were compared to growth and life for monolithic specimens.

Through-the-Thickness Crack Growth

The da/dN data from CT specimens were plotted versus ΔK using equation (1). All of the compact data were generated at a stress ratio, R, of 0.1. A curve was drawn through the mean of the da/dN versus ΔK data points for each of the three material systems. The plot is shown in Fig. 3. On the average, the 6-ply laminate had a 20 percent slower crack growth rate than the monolith. The single ply had a crack growth rate 15 percent slower than the laminate.

When calculating the stress-intensity factors, the laminate's material thickness was considered to consist of the titanium plies only. That is to say, the thickness for the laminated plate was assumed to be 7.62 mm. Since the modulus of the adhesive is approximately 30 times less than the modulus of titanium, the titanium was assumed to carry all of the load.

Fracture Toughness Tests

After the cracks in the compact specimens were grown to predetermined crack lengths, the specimens were pulled statically to failure. The critical failing loads, P_c, were recorded. The fracture toughness, K_c, was then calculated using equation (1b). The results for the three material systems are presented in Fig. 4.

The crack lengths at which the specimens were pulled to failure are indicated at the top of each bar. All three material systems were tested at a crack length of 62 mm. The toughness, measured from the laminate (again using only the titanium thicknesses in the calculation of K_c), is the same as for the individual plies. Each ply in the laminate failed at approximately a 45-deg slant, indicating a plane-stress type failure. This agrees with earlier reports on aluminum [2]. Each ply fails independently. The fracture surface of the thick monolith implied near plane-strain failure conditions (small shear lips).

When tested with a crack length $a = 62$ mm, the laminate toughness was 36 percent higher than the monolith with the same crack length. For tests with $a = 49$ mm, the laminate toughness was 41 percent higher.

The laminated specimens averaged 39 percent tougher than the monolithic compact specimens. To examine what this higher toughness would mean in a practical situation, two identical structures were assumed, one monolithic and one laminated, loaded such that the titanium material was under the same applied stress. Both structures had through-the-thickness cracks. The critical stress-intensity, K_c, is given by

$$K_c = S(\pi a)^{1/2} f \qquad (9)$$

where

S = remotely applied stress

f = boundary correction factor

If both structures have the same stress and shape, S and f are the same for each. Consequently, since

$$\frac{K_c^{LAM}}{K_c^{MON}} = 1.39 \Rightarrow \left(\frac{a^{LAM}}{a^{MON}}\right)^{1/2} = 1.39 \tag{10}$$

This implies $a^{LAM} = 1.93a^{MON}$. Thus, a through-the-thickness crack in the laminated structure can grow almost twice as long as a through-the-thickness crack in a monolithic structure under the same applied stress before the structure fails.

The fracture toughness is higher in the laminate because each ply fails independently as if in a plane-stress state. Fig. 5(a) shows an edge view of the fracture surface of the laminated compact specimen; each ply has a shear lip. These shear lips are like those shown in Ref. 2 for aluminum. The fracture toughness improvement found herein for the laminated titanium is somewhat lower than the improvement reported by Kaufman [2] and Alic [3] for laminated aluminum and by Sloter and Petersen [20] for metal-metal laminates of titanium.

Crack growth rates for through-the-thickness cracks in laminated compact specimens are markedly slower than rates in monolithic materials. The 20 percent reduction in crack growth rate (Fig. 3) and almost twice the critical crack length makes laminated titanium much more damage tolerant than monolithic.

Fig. 5(b) shows the fatigue crack front in the compact specimen. Each ply has a curved crack front and the crack grows uniformly across the laminate. The crack in each ply grows somewhat independently, which explains why they grow more slowly than they do in the thick monolithic plate. But they do not grow as slow as they do in an individual ply. Schijve, et al. [6] showed that the through-the-thickness crack growth rates in laminated Alclad aluminum are closer to that of the individual ply growth rates than reported in Fig. 3 for Ti-6Al-4V. Schijve also showed that the growth rate in laminated Alclad slowed by 50 percent, compared to a slowing of 20 percent for the Ti-6Al-4V. Pfeiffer and Alic [21] reported no obvious improvement in through-the-thickness crack growth for laminated 7075-T6 aluminum over a monolith of the same thickness.

Thin Sheet Crack Growth

To predict laminate crack growth, the crack growth rate behavior of single plies must be known. Thin sheet CCT specimens were tested at three stress ratios. Equation (2) defined ΔK. The data for da/dN against ΔK are presented in Fig. 6 for stress ratios of 0.7, 0.3, and 0.1. The solid curves show how well equation (3) fits the data. The constants used in equation (3) are $\Delta K^{o}_{TH} = 8.8$ MPa$\sqrt{m}$, $K_c = 110$ MPa$\sqrt{m}$, $C = 2.78 \times 10^{-3}$, and $n = 0.955$. Crack growth rate is given in mm/cycle.

Laminate Damage Tolerance

Surface-cracked tension specimens of both the laminated and monolithic materials were tested. Each had an initial semicircular surface crack 5 mm long. The crack in the laminate was only in one outer ply. Fig. 7 compares the crack growth behavior of two laminated and two monolithic specimens under constant-amplitude loading at $R = 0.1$. The maximum load in the monolith and laminate was 172 kN and 139 kN, respectively. The crack in the monolithic specimens grew slowly at first, then accelerated until the specimen failed at approximately $a = 23$ mm. The crack in the laminate grew faster at the start, but did not accelerate nearly as much.

The stress-intensity factor for this laminate with a small through-crack (2a = 5 mm) in an outer ply was approximately (f_ℓ is assumed to be 1.0)

$$\Delta K = \Delta S(\pi a)^{1/2} = 228 \text{ MPa}(\pi\ 0.0025)^{1/2} = 20.2 \text{ MPa}\sqrt{m} \qquad (11)$$

The stress-intensity factor for a semicircular surface crack (2a = 5 mm) in the monolith was approximately

$$\Delta K = \Delta S\left(\frac{\pi a}{Q}\right)^{1/2} = 217 \text{ MPa}\left(\frac{\pi\ 0.0025}{2.5}\right) = 12.7 \text{ MPa}\sqrt{m} \tag{12}$$

Since the monolith's surface crack had the lower stress-intensity factor range, the monolith's crack growth rate was lower. The relative crack growth rates were approximated by equation (3), with the data from Fig. 6. The ratio of the growth rates of the laminate's crack to the monolith's crack was approximately 3.6. This ratio corresponded to that measured experimentally during the initial growth rate period of the two cracks. The $f_{\ell} = 1.0$ assumption will be discussed later.

The crack in the laminate grew across the entire width of the specimen. But this did not cause failure; the remaining plies supported the load. Fig. 8 shows the relative life of each of the specimens. The life of a flawed specimen will be referred to herein as the damage tolerance life. The laminated specimen survived an additional 200,000 cycles after the outer ply had completely cracked across the width. The life of only one of the two laminated specimens tested (under constant-amplitude loading) is reported in Fig. 7 because the other specimen failed in the grip area.

The algorithm described in equations (4) through (8) was used to predict, for constant-amplitude loads, the crack growth in the outer ply of the laminated titanium CCT specimen. A value of 1.0 for the f_{ℓ} term in equation (8) best predicted the crack growth behavior, as shown in Fig. 7. The value of 1.0 implies that the adhesive had negligible constraint effect on the crack growth. The aluminum laminates analyzed in Refs. 4 and 5 also used AF-147 adhesive. But there a value of $f_{\ell} = 0.62$ was needed to correlate the crack growth data. Why the adhesive influenced the crack growth more (slowing it down) in the aluminum than in the titanium laminates is unknown at this time.

Specimens identical to the ones tested under constant-amplitude loading were tested under a typical fighter aircraft spectrum loading. The spectrum was M-90, reported in Ref. 23, with the compressive loads deleted. The maximum load for the spectra was 222 kN for the monolith and 180 kN for the laminate (equal load-to-weight ratio). Fig. 10 presents crack growth versus number of cycles for both the monolithic and laminated specimen. One outer ply of the laminated specimen was initially cracked. Again, initially the crack growth rate in the laminate was higher than that in the monolith, but the crack growth rate in the monolith eventually surpassed the one in the laminate and the monolith failed at $a = 25$ mm; the crack in the outer ply of the laminate grew across the width of the specimen. The laminated specimens were fatigued until the number of applied blocks of spectrum loadings was 15 times the number required to fail the monolith; since the laminated specimen still had not failed, the tests were terminated. The relative fatigue lives are shown in Fig. 11. The laminated specimen developed a crack in the outer ply opposite the one containing the initial flaw. This crack grew completely through the back ply and across the width of the specimen at approximately 3000 blocks of spectrum loading. But even with two out of six plies completely cracked, the specimen carried the load.

The tolerance-to-surface damage, as is illustrated in Figs. 6 through 11, was superior in a laminated plate. For specimens containing the same size initial crack, the cyclic life was much longer for the laminate than in the monolith. For example, compare the number of cycles required for the laminate's surface crack length to reach the monolith's failing crack length to the number of cycles at which the monolith failed for the tests shown in Figs. 7 and 10. This relative increase in number of cycles (from 30 to 60 percent) is expected under spectrum loads because the individual plies of the laminate are in plane stress, which allows for large (relative to plane-strain conditions of the thick monolith) crack-tip plastic zone radii to develop. These large plastic zone radii retard crack growth [17], and thus slow crack growth under some spectrum loading.

A laminated specimen with an initial semicircular surface crack large enough to extend into the first two outer plies was tested under the previously described spectrum. Fig. 12 shows the crack growth for both the laminated and monolithic specimen; the surface crack started at a size $a = 5$ mm. Again the monolith failed at approximately $a = 25$ mm, while the laminate crack grew across the entire width of the specimen. Both of the initially flawed plies cracked all the way across the width at approximately the same time. The laminate specimen continued to cycle for 2420 more blocks of cyclic loading (15 times the life of the monolithic specimen) without failure; the test was then terminated. Fig. 13 indicates the relative lives of the monolithic and laminated specimens.

Number of Plies Considerations

This study did not experimentally address the effects of varying the number of plies in the laminate. However, a criterion for determining an optimum number of plies will be discussed. A crack in an outer ply rarely induces a crack in an adjacent ply. For spectrum loading, the laminate containing surface cracks in one or two plies lasted over 15 times longer than the similarly flawed monolith. The reason for this long life is simple. After the ply completely cracked across the width of the specimen, the remaining plies were like an unnotched fatigue coupon. The fatigue limit (10^7 cycles) for sheet Ti-6Al-4V at $R = 0$ from Ref. 24 is a maximum stress of 560 MPa. The maximum laminate spectrum stress was 233 MPa. This maximum stress occurs only once per block. The root-mean-square (rms) value of the maximum stress of a block of the spectrum was 110 MPa. The rms value of a spectrum has been shown to be an approximate method for assessing the fatigue and crack growth [25] damage. If one or two plies of the six-ply laminate were lost, the resulting rms maximum stress in the remaining five or four plies would be 132 MPa and 165 MPa, respectively. These values are well below the 560 MPa fatigue limit, so very long life may be expected.

The constant-amplitude test reported in Fig. 7 had a maximum laminate stress of 266 MPa at $R = 0.1$. The fatigue limit (10^7 cycles) for $R = 0.1$ is a maximum stress of 520 MPa [21]. If an outer ply cracked across the width of the specimen, the stress on the remaining five plies would be 319 MPa. This stress is still well below the fatigue limit, but the specimen failed at approximately 290,000 cycles. The laminate plies were not polished like typical unnotched fatigue coupons that are normally used to develop S-N type fatigue data. Furthermore, load is transferred between the cracked and unbroken plies and causes local stress concentration. Fatigue is often a function of free surface area per volume; the greater the surface area, the greater the chance for fatigue crack initiation. Therefore, laminated structures may be worse than monoliths from a fatigue initiation criterion. Even so, the laminate is clearly superior to the monolith from a damage propagation and fracture standpoint.

To determine how many plies should be in a laminate of given thickness, the operational load level and the type of damage expected must be considered. The number of plies should be such that when one or two outer plies are lost to damage, the remaining plies are stressed well below their fatigue limit.

CONCLUSIONS

The fracture toughness was increased and crack growth rates of titanium were lowered by laminating thin sheets of titanium with adhesives. The titanium laminates proved to be much more damage tolerant than titanium plate of the same thickness. The through-the-thickness fracture toughness was improved 39 percent; this implies that a laminate can sustain the same load as a monolith, yet contain a through-crack almost twice as long as that in a monolith. Through-the-thickness crack growth rates were 20 percent lower in the laminate than in the monolith. The laminate's damage tolerance life superiority was even greater under spectrum loading because the thin plies of the laminate were more sensitive to retardation than was the thick monolithic plate. The damage tolerance life of the surface-cracked laminate was 6 to over 15 times the life of a monolithic specimen.

A simple algorithm is presented to predict crack growth in a cracked outer ply of a laminate. The analytical crack growth prediction fits the experimental data extremely well.

The findings of this report along with previously referenced research on aluminum show that adhesive lamination improved the basic fracture mechanics properties of relatively thick plate material.

REFERENCES

[1] Elber, W., and Davidson, J. R., "A Material Selection Method Based on Material Properties and Operating Parameters," NASA TN D-7221, National Aeronautics and Space Administration, Apr. 1973.

[2] Kaufman, J. G., "Fracture Toughness of 7075-T6 and -T761 Sheet, Plate, and Multi-Layered Adhesive-Bonded Panels," Journal of Basic Engineering, Trans. ASME, Series D, Vol. 89, Sept. 1967, pp. 503-507.

[3] Alic, J. A., "Stable Crack Growth in Adhesively Bonded Aluminum Alloy Laminates," International Journal of Fracture, Vol. 11, No. 4, Aug. 1975, pp. 701-704.

[4] Johnson, W. S., and Stratton, J. M., "Effective Remote Stresses and Stress Intensity Factors for an Adhesively Bonded Multi-Ply Laminate," Engineering Fracture Mechanics, Vol. 9, No. 2, 1977, pp. 411-421.

[5] Johnson, W. S., Rister, W. C., and Spamer, T., "Spectrum Crack Growth in Adhesively Bonded Structure," Journal of Engineering Materials and Technology, ASME, Vol. 100, Jan. 1978, pp. 57-63.

[6] Schijve, J., et al., "Fatigue Properties of Adhesive-Bonded Laminated Sheet Material of Aluminum Alloys," Engineering Fracture Mechanics, Vol. 12, No. 4, 1979, pp. 561-579.

[7] Maris, J. L., and Kuhn, G. E., "Advanced Technology Wing Structure," AFWAL-TR-80-3031, Air Force Wright Aeronautical Laboratories, May 1980.

[8] McClaren, S. W., Maris, J. L., and Ely, R. A., "Advanced Wing Box Evaluations," AFWAL-TR-80-3033, Air Force Wright Aeronautical Laboratories, Apr. 1980.

[9] Potter, D. L., et al., "Primary Adhesively Bonded Structures Technology (PABST) Design Handbook for Adhesive Bonding," AFFDL-TR-79-3129, Air Force Flight Dynamics Laboratory, Nov. 1979.

[10] Irving, R. R., "A Tale of Adhesively Bonded Aircraft," Iron Age, May 4, 1981, pp. 87-88.

[11] Schliekelmann, R. J., "Past, Present, and Future of Structural Adhesive Bonding in Aero-Space Applications," Trans. Japan Society for Composite Materials, Vol. 5, No. 1/2, Dec. 1979, pp. 1-13.

[12] "Standard Test Method for Constant-Load-Amplitude Fatigue Crack Growth Rates Above 10^{-8} m/cycle," ASTM Standard E647-81, American Society for Testing and Materials.

[13] "Standard Test Method for Plane-Strain Fracture Toughness of Metallic Materials," ASTM Standard E399-81, American Society for Testing and Materials.

[14] Tada, H., Paris, P. C., and Irwin, G. R., "The Stress Analysis of Cracks Handbook," Del Research Corporation, 1973.

[15] Forman, R. G., Kearney, V. C., and Engle, R. M., "Numerical Analysis of Crack Propagation in Cyclic-Loaded Structures," Journal of Basic Engineering, Trans. ASME, Series D, Vol. 89, No. 3, Sept. 1967, pp. 459-464.

[16] Chu, H. P., "Effect of Mean Stress Intensity on Fatigue Crack Growth in a 5456-H117 Aluminum Alloy," Fracture Toughness and Slow Stable Cracking, ASTM STP 559, American Society for Testing and Materials, 1974, pp. 245-263.

[17] Johnson, W. S., "Multi-Parameter Yield Zone Model for Predicting Spectrum Crack Growth," Methods and Models for Predicting Fatigue Crack Growth Under Random Loading, ASTM STP 748, American Society for Testing and Materials, 1981, pp. 85-102.

[18] Roderick, G. L., "Prediction of Cyclic Growth of Cracks and Debonds in Aluminum Sheets Reinforced with Boron/Epoxy," Fibrous Composites in Structural Design, Plenum, 1980, pp. 467-481.

[19] Ratwani, M. M., "Characterization of Fatigue Crack Growth in Bonded Structures," Crack Growth Prediction in Bonded Structures, Vol. 1, AFFDL-TR-77-31, Air Force Flight Dynamics Laboratory, June 1977.

[20] Sloter, L. E., and Petersen, D. H., "Fracture and Fatigue of Metal-Metal Laminates," Proceedings of the 26th National SAMPE Symposium, Apr. 1981, pp. 313-324.

[21] Pfeiffer, N. J., and Alic, J. A., "Fatigue Crack Propagation in 8- and 22-Layer 7075-T6 Aluminum Alloy Laminates," Journal of Engineering Materials and Technology, ASME, Vol. 100, Jan. 1978, pp. 32-38.

[22] Stratton, J. M., and Jones, R. L., "Fatigue and Fracture Characteristics of Adhesively Bonded 2024-T81 Aluminum Laminates," ERR-FW-1584, General Dynamics, Dec. 1974.

[23] Chang, J. B., "Round-Robin Crack Growth Predictions on Center-Cracked Tension Specimens Under Random Spectrum Loading," Methods and Models for Predicting Fatigue Crack Under Random Loading, ASTM STP 748, American Society for Testing and Materials, 1981, pp. 3-40.

[24] Ruff, P. E., "Metrication of Mil-HDBK-5C," AFWAL-TR-80-4110, Air Force Wright Aeronautical Laboratories, Aug. 1980.

[25] Hudson, C. M., "A Root-Mean-Square Approach for Predicting Fatigue Crack Growth Under Random Loading," Methods and Models for Predicting Fatigue Crack Under Random Loading, ASTM STP 748, American Society for Testing and Materials, 1981, pp. 41-52.

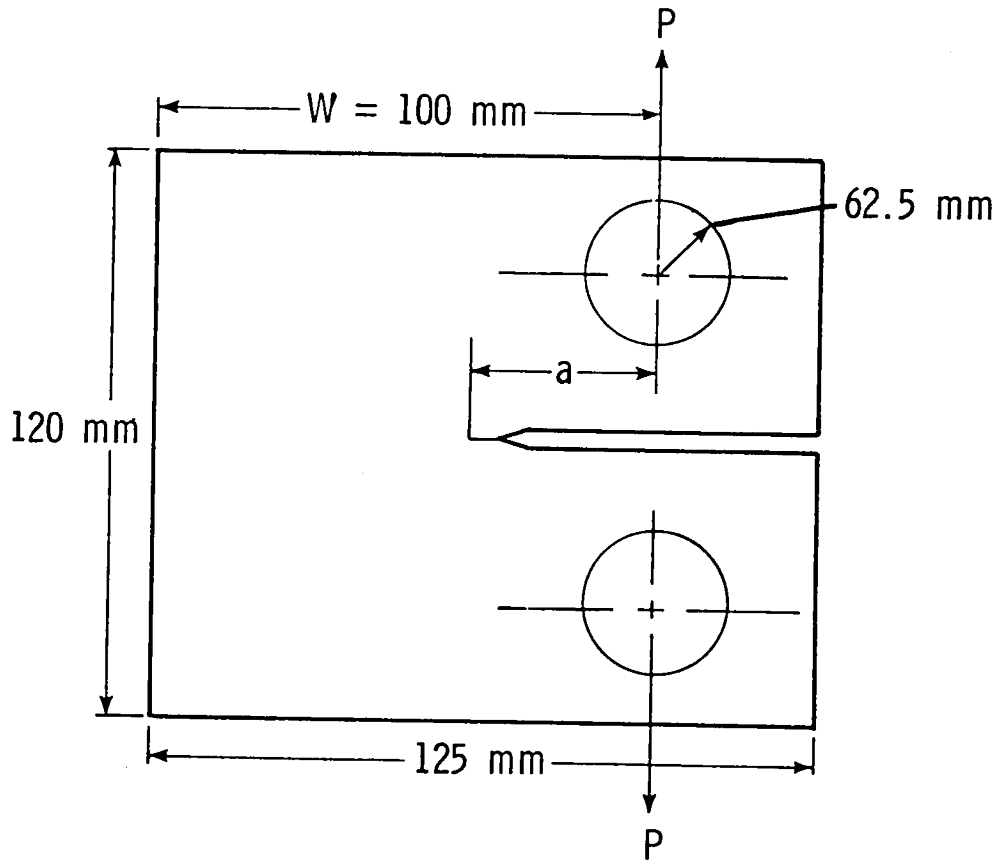

Fig. 1 Compact specimen (CT).

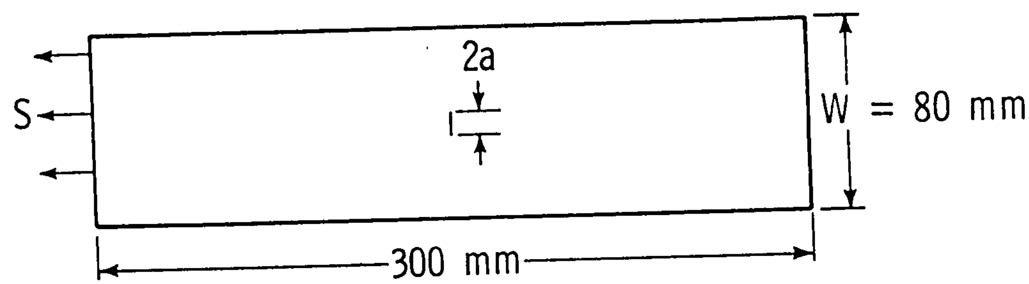

Fig. 2 Center-cracked tension specimen (CCT).

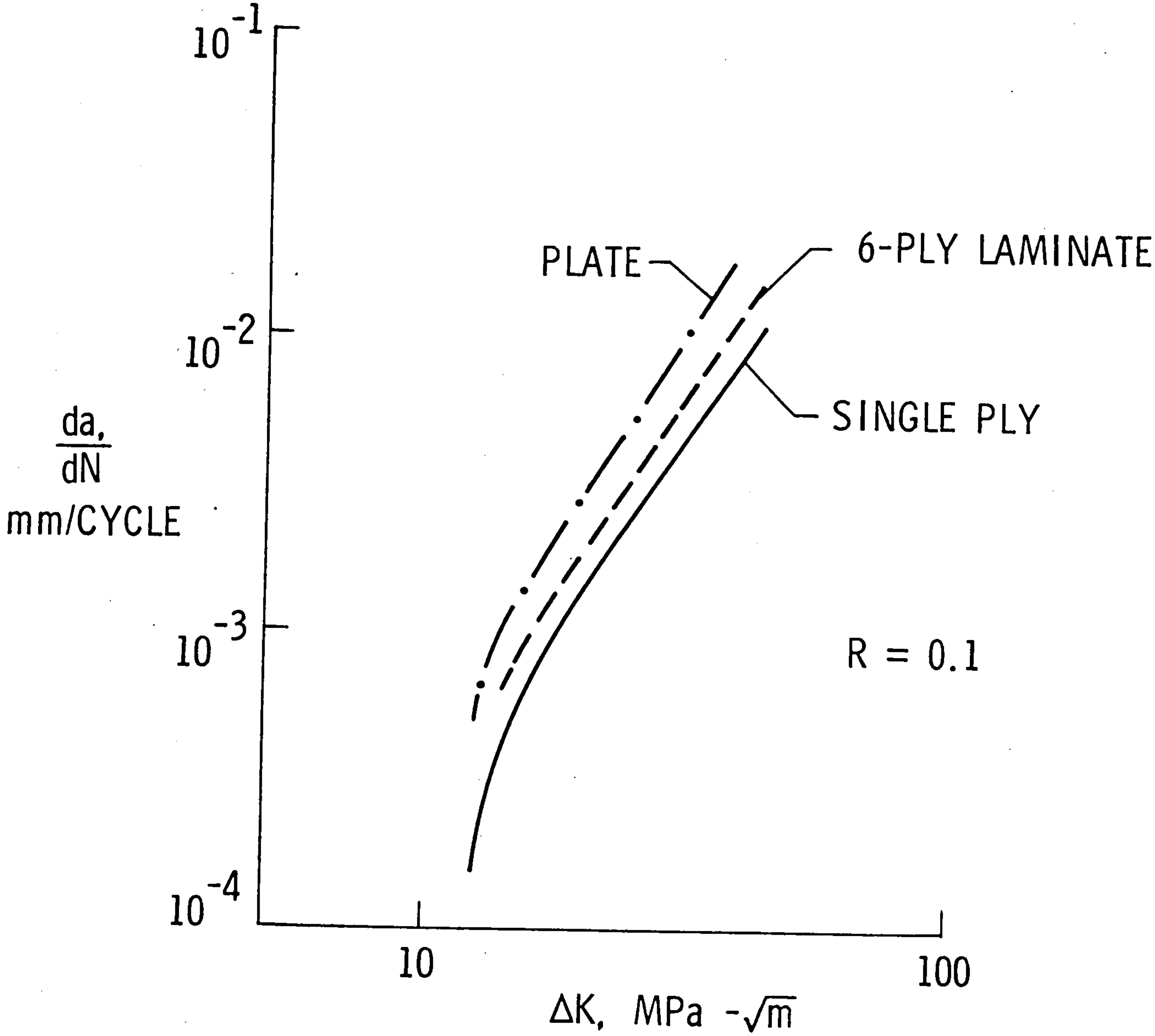

Fig. 3 Through-the-thickness crack growth rate data for Ti-6Al-4V.

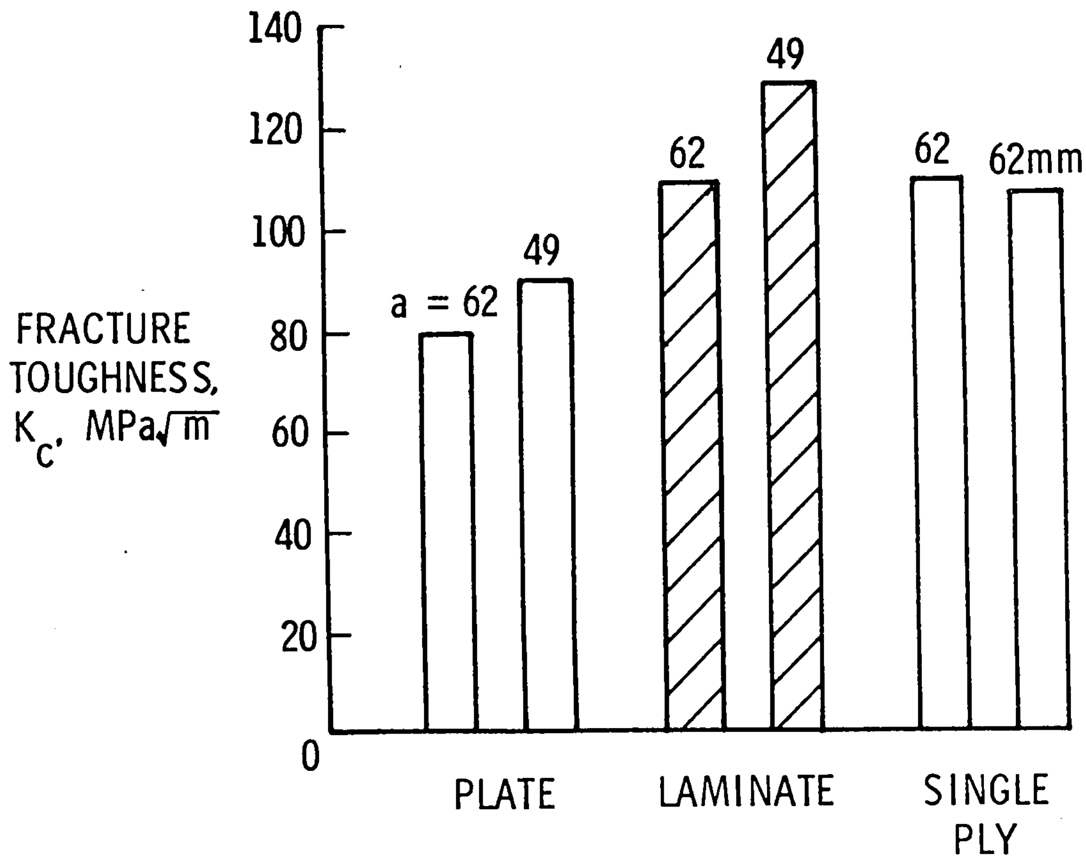

Fig. 4 Fracture toughness of Ti-6Al-4V plate, laminate, and thin sheet (single ply).

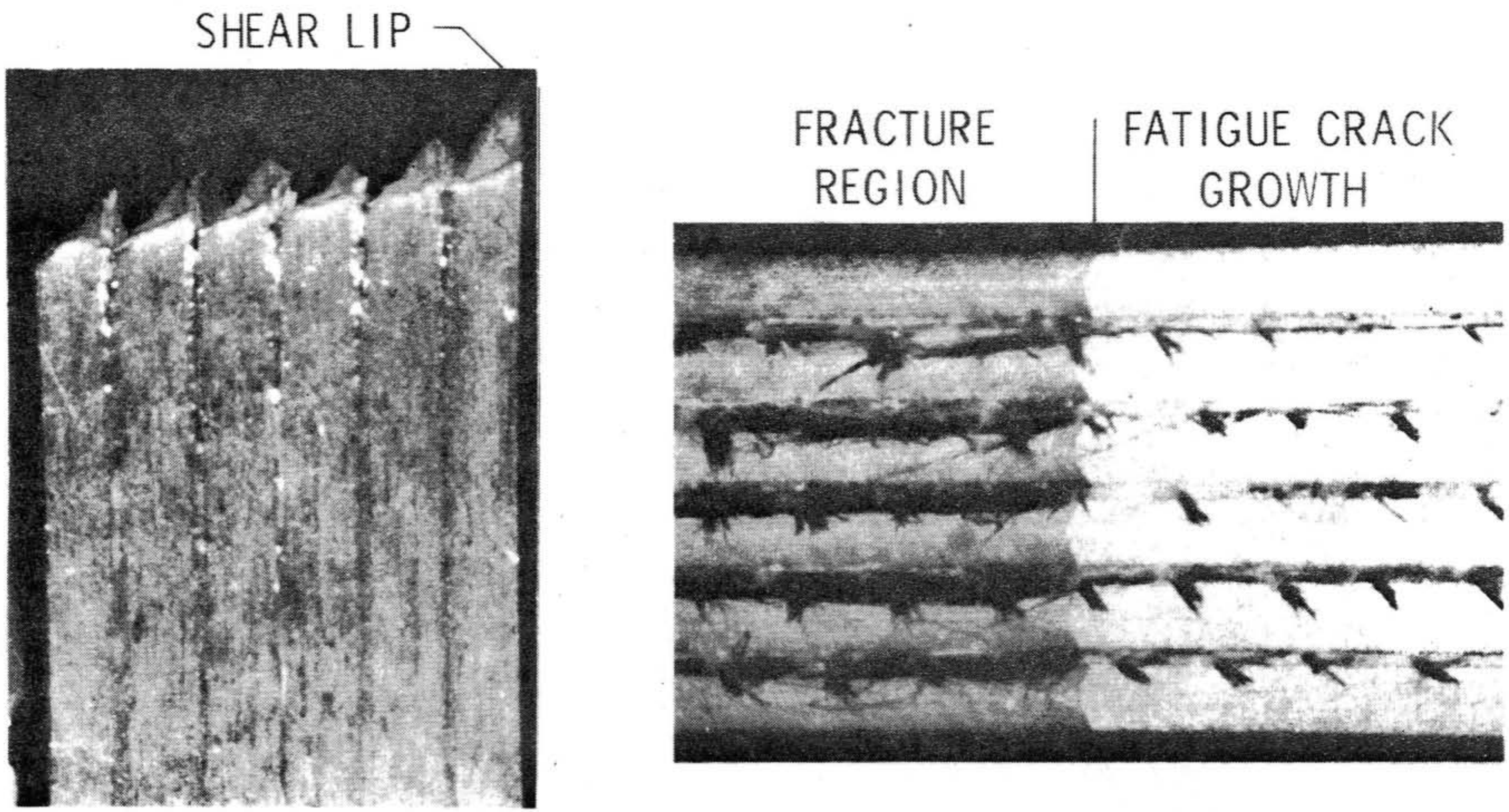

(a) EDGE VIEW OF FRACTURE SURFACE

(b) FATIGUE CRACK GROWTH FRONT

Fig. 5 Failure surfaces of adhesively laminated Ti-6Al-4V. The thread-like material in the photomicrographs are scrim cloth fibers from the adhesive bondline.

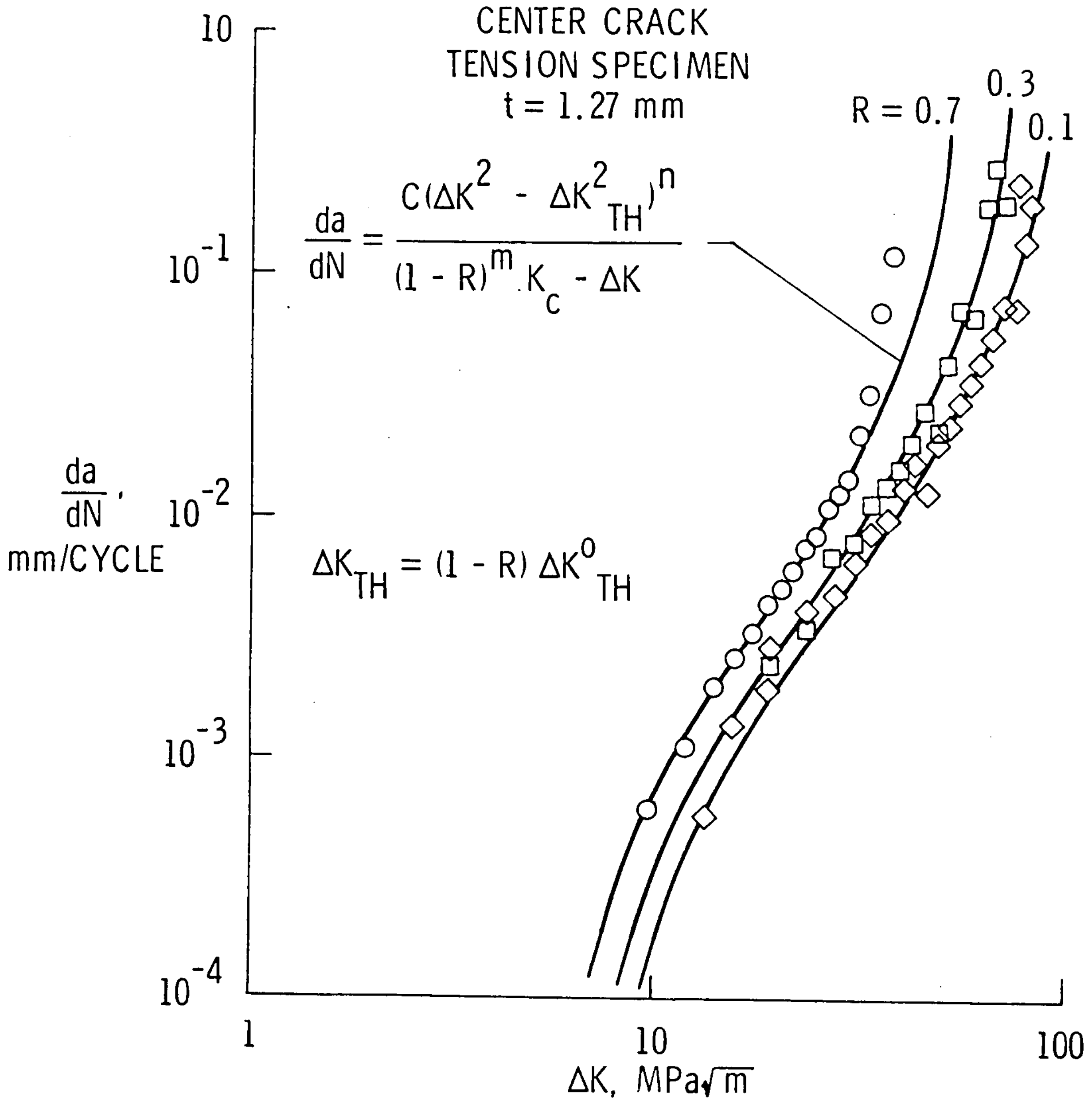

Fig. 6 Crack growth rate data for Ti-6Al-4V sheet, 1.27 mm thick.

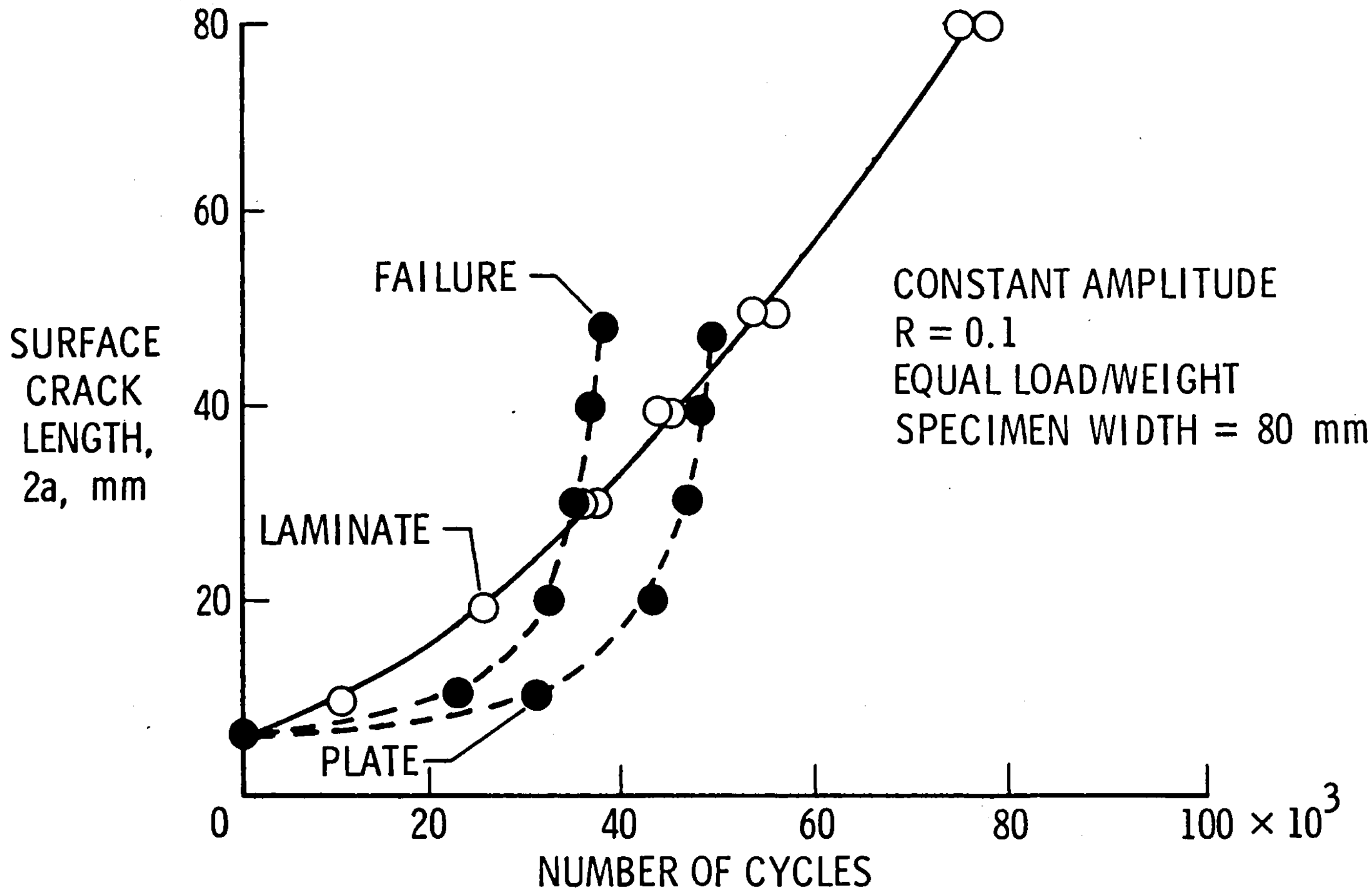

Fig. 7 Crack growth data from surface cracks in Ti-6Al-4V subjected to constant-amplitude loads.

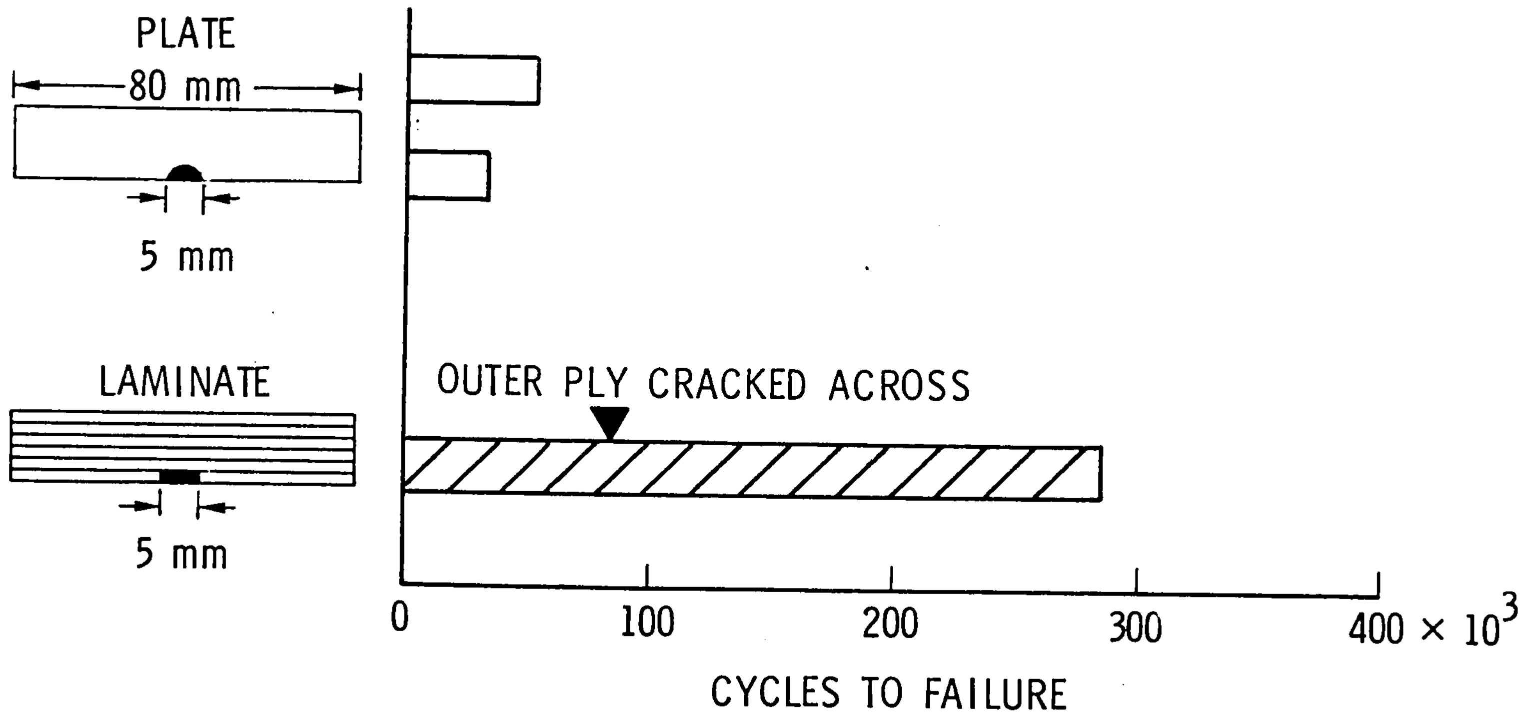

Fig. 8 Damage tolerant lives of surface-cracked Ti-6Al-4V specimens subjected to constant-amplitude loading.

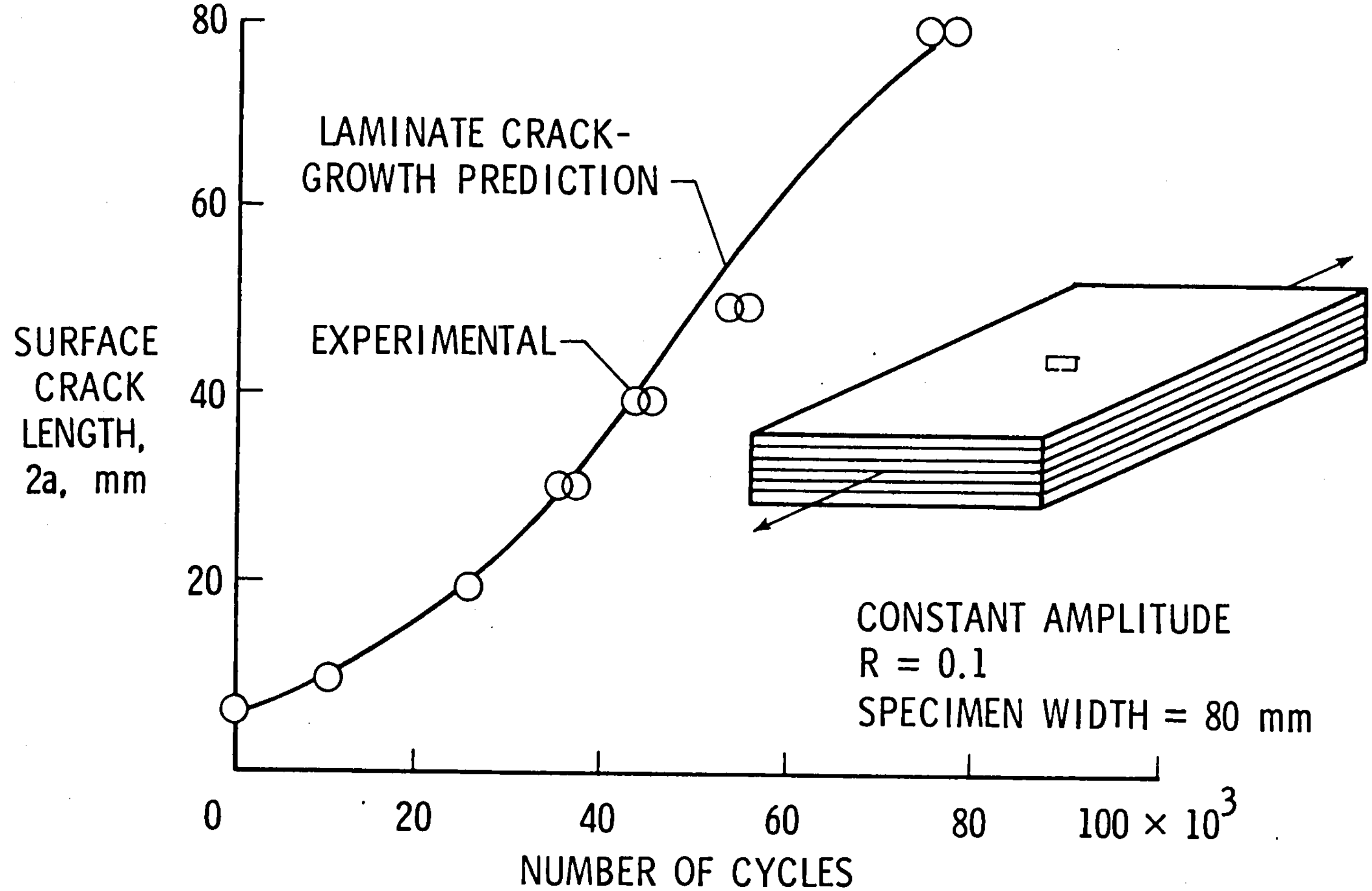

Fig. 9 Comparison of predicted and test results for a crack growing in a Ti-6Al-4V laminated ply.

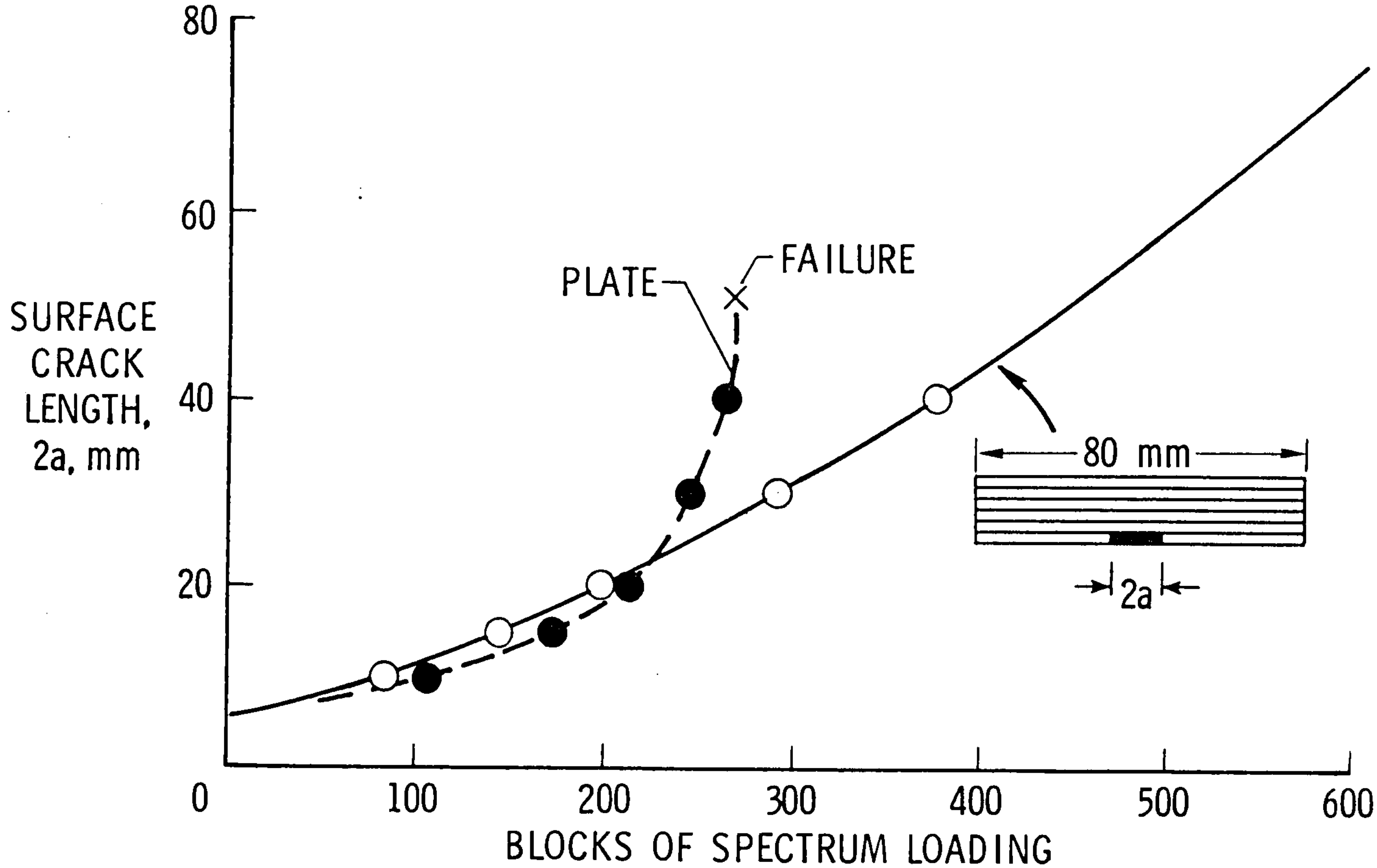

Fig. 10 Surface crack growth in Ti-6Al-4V subjected to spectrum loads.

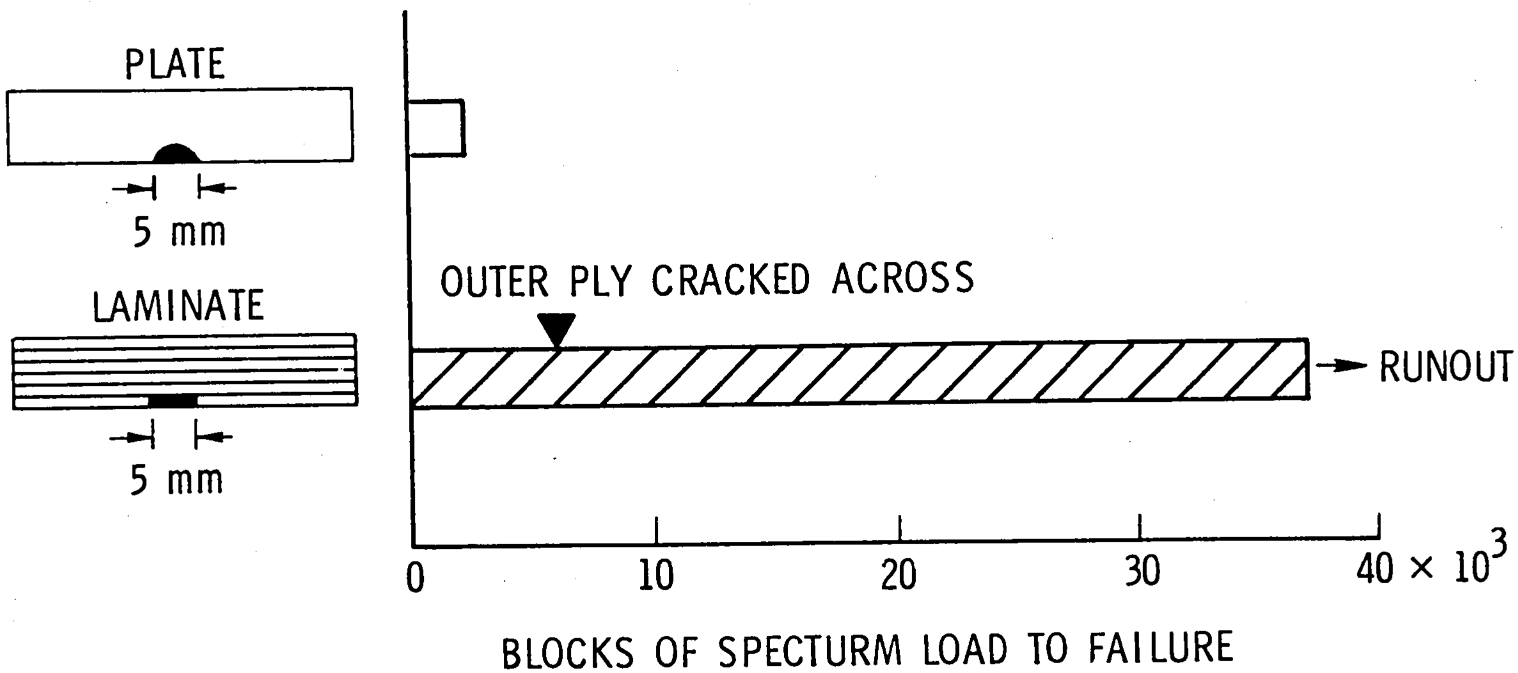

Fig. 11 Damage tolerant lives of surface-cracked Ti-6Al-4V specimens subjected to spectrum loading.

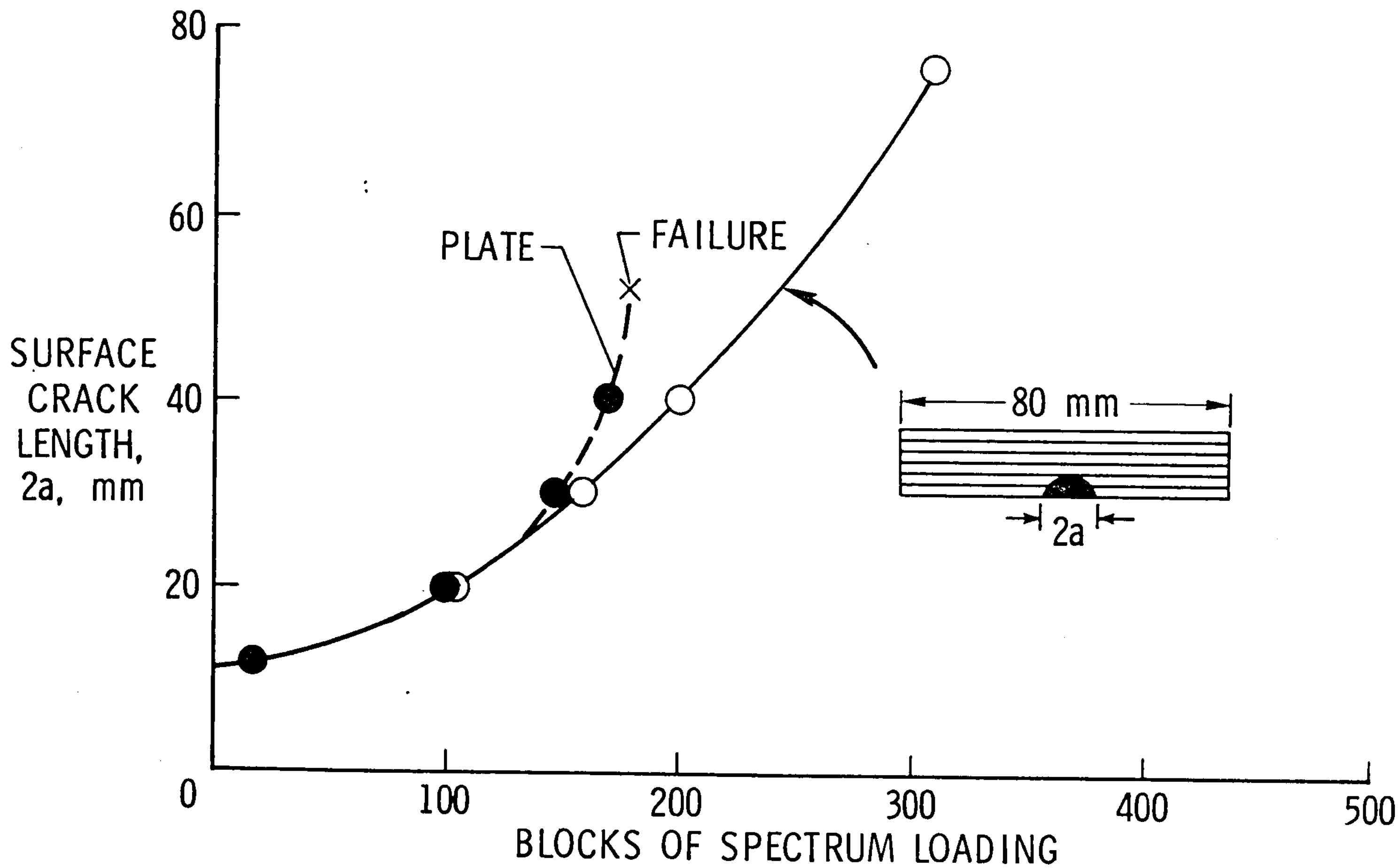

Fig. 12 Surface crack growth in Ti-6Al-4V subjected to spectrum loads.

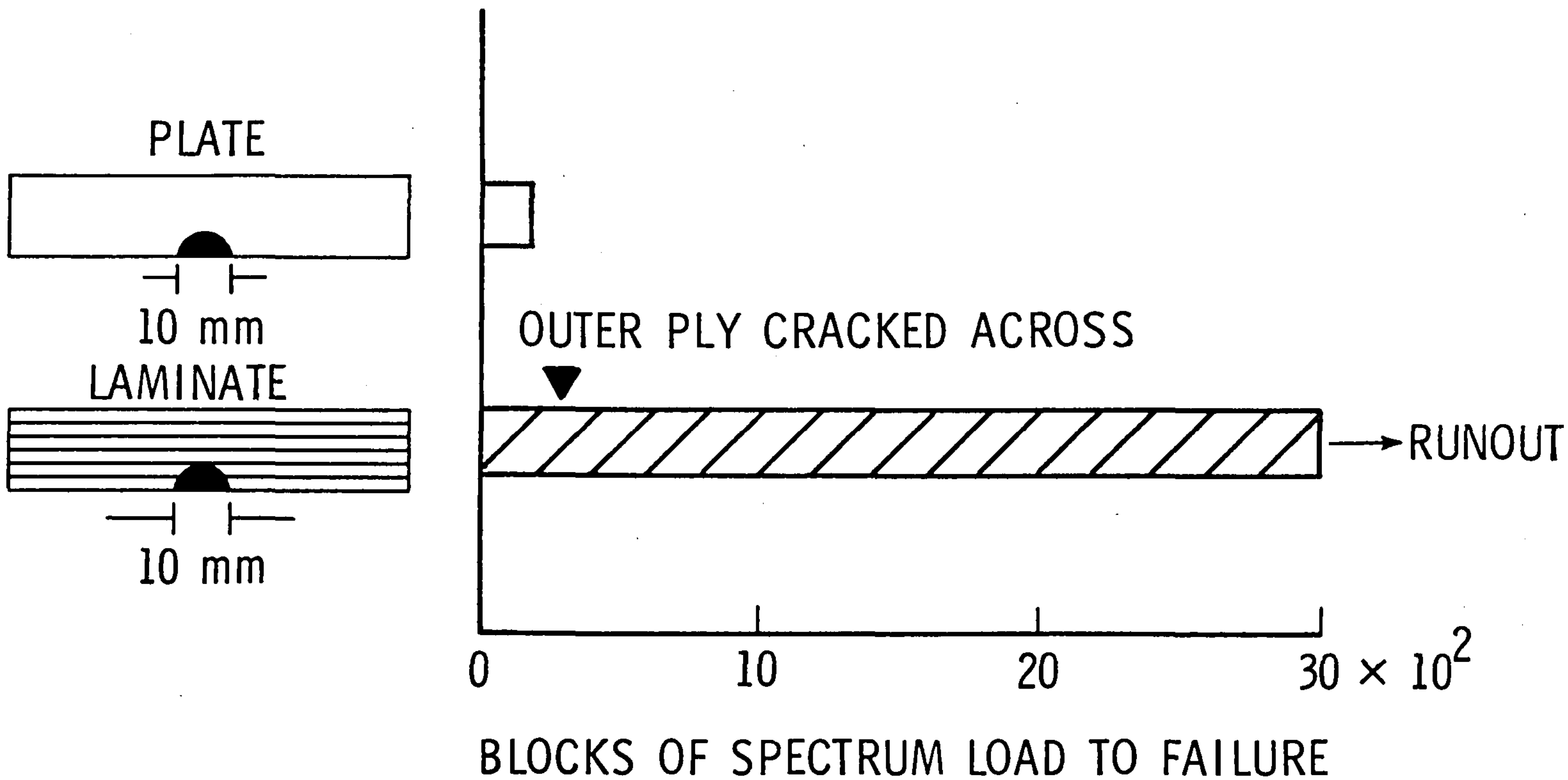

Fig. 13 Damage tolerant lives of surface-cracked Ti-6Al-4V specimens subjected to spectrum loading.

1. Report No. NASA TM-84525	2. Government Accession No.	3. Recipient's Catalog No.

4. Title and Subtitle
IMPROVED DAMAGE TOLERANCE OF TITANIUM BY ADHESIVE LAMINATION

5. Report Date
July 1982

6. Performing Organization Code
505-33-23-02

7. Author(s)
W. S. Johnson

8. Performing Organization Report No.

9. Performing Organization Name and Address
NASA Langley Research Center
Hampton, VA 23665

10. Work Unit No.

11. Contract or Grant No.

12. Sponsoring Agency Name and Address
National Aeronautics and Space Administration
Washington, DC 20546

13. Type of Report and Period Covered
Technical Memorandum

14. Sponsoring Agency Code

15. Supplementary Notes Presented at the 23rd AIAA/ASME/ASCE/AHS Structures, Structural Dynamics, and Materials Conference, New Orleans, Louisiana, May 10-12, 1982. This paper has been submitted for publication in the ASME Journal of Engineering Materials and Technology.

16. Abstract

Basic damage tolerance properties of Ti-6Al-4V titanium plate can be improved by laminating thin sheets of titanium with adhesives. Compact tension and center-cracked tension specimens made from thick plate, thin sheet, and laminated plate (six plies of thin sheet) were tested. The fracture toughness of the laminated plate was 39 percent higher than the monolithic plate. The laminated plate's through-the-thickness crack growth rate was about 20 percent less than that of the monolithic plate. The damage tolerance life of the surface-cracked laminate was 6 to over 15 times the life of a monolithic specimen. A simple method of predicting crack growth in a crack ply of a laminate is presented.

17. Key Words (Suggested by Author(s))	18. Distribution Statement
Adhesive bonding Titanium Fracture mechanics Fatigue crack growth Laminated metals	Unclassified - Unlimited Subject Category 39

19. Security Classif. (of this report)	20. Security Classif. (of this page)	21. No. of Pages	22. Price*
Unclassified	Unclassified	34	A03

* For sale by the National Technical Information Service, Springfield, Virginia 22161